

Therapeutic effect of apatinib-loaded nanoparticles on diabetes-induced retinal vascular leakage

Ji Hoon Jeong^{1,*}
Hong Khanh Nguyen^{2,*}
Jung Eun Lee¹
Wonhee Suh²

¹School of Pharmacy, Sungkyunkwan University, Suwon, ²College of Pharmacy, Chung-Ang University, Seoul, Korea

*These authors contributed equally to this work

Abstract: Apatinib, a novel and selective inhibitor of vascular endothelial growth factor (VEGF) receptor 2, has been demonstrated recently to exhibit anticancer efficacy by inhibiting the VEGF signaling pathway. Given the importance of VEGF in retinal vascular leakage, the present study was designed to investigate whether apatinib-loaded polymeric nanoparticles inhibit VEGF-mediated retinal vascular hyperpermeability and block diabetes-induced retinal vascular leakage. For the delivery of water-insoluble apatinib, the drug was encapsulated in nanoparticles composed of human serum albumin (HSA)-conjugated polyethylene glycol (PEG). In vitro paracellular permeability and transendothelial electric resistance assays showed that apatinib-loaded HSA-PEG (Apa-HSA-PEG) nanoparticles significantly inhibited VEGF-induced endothelial hyperpermeability in human retinal microvascular endothelial cells. In addition, they substantially reduced the VEGF-induced junctional loss and internalization of vascular endothelial-cadherin, a major component of endothelial junction complexes. In vivo intravitreal injection of Apa-HSA-PEG nanoparticles in mice blocked VEGF-induced retinal vascular leakage. These in vitro and in vivo data indicated that Apa-HSA-PEG nanoparticles efficiently blocked VEGF-induced breakdown of the blood–retinal barrier. In vivo experiments with streptozotocin-induced diabetic mice showed that an intravitreal injection of Apa-HSA-PEG nanoparticles substantially inhibited diabetes-induced retinal vascular leakage. These results demonstrated, for the first time, that apatinib-loaded nanoparticles may be a promising therapeutic agent for the prevention and treatment of diabetes-induced retinal vascular disorders.

Keywords: permeability, retinal vascular endothelial cells, vascular endothelial growth factor

Introduction

In normal retinas, endothelial cells at the blood–retinal barrier (BRB) are tightly sealed by complex intercellular junctions that restrict the entry of molecules into the inner retina and protect retinal neural tissue from harmful substances present in the blood. However, these barrier properties of the retinal vasculature are disrupted during the early pathogenesis of diabetic retinopathy, resulting in enhanced retinal vascular leakage.¹ Because this vascular leakage leads to the development of edema in the macular visual field, which is the main cause of vision loss in patients with diabetes, many efforts have been made to develop effective therapeutic strategies to inhibit retinal vascular leakage.

Vascular endothelial growth factor (VEGF) plays a crucial role in the pathological processes of the BRB breakdown and macular edema in diabetic patients.² Among many VEGF receptor (VEGFR) subtypes, VEGFR2 is most commonly implicated in the VEGF-induced pathological formation of a leaky vasculature.³ VEGF-induced phosphorylation of VEGFR2 disrupts the endothelial cell–cell junction through various mechanisms. Among these, VEGF/VEGFR2 signaling can induce the internalization of

Correspondence: Wonhee Suh
College of Pharmacy, Chung-Ang University, 84 Heukseok-Ro, Dongjak-gu, Seoul 06974, Korea
Tel +82 2 820 5960
Fax +82 2 816 7338
Email wsuh@cau.ac.kr

vascular endothelial (VE)-cadherin, consisting of endothelial junction complexes, which then leads to the disassembly of endothelial junction complexes.⁴ Anti-VEGF agents, such as ranibizumab and aflibercept, have recently shown substantial therapeutic efficacy in halting disease progression and improving the vision of diabetic patients.⁵

Apatinib is a novel receptor tyrosine kinase inhibitor that selectively targets VEGFR2.⁶ It prevents VEGF-induced phosphorylation of VEGFR2 and the subsequent downstream signaling responsible for the biological effects of VEGF. Preclinical studies have shown that apatinib significantly reduced tumor growth in several established human tumor xenograft models by inhibiting tumor-induced angiogenesis.⁷ In clinical trials, apatinib exhibited antitumor activity in patients with gastric cancer.^{6,8,9} In this regard, we propose that apatinib may also be effective in inhibiting VEGF-induced retinal vascular hyperpermeability and have beneficial actions against the diabetes-induced breakdown of the BRB.

Because apatinib is insoluble in water, we encapsulated it in nanoparticles composed of human serum albumin (HSA)-conjugated polyethylene glycol (PEG) to avoid accumulation of the insoluble drug in the vitreous cavity, which is often associated with ocular toxicity. In the present study, we showed that intravitreal injection of apatinib-loaded nanoparticles could prevent diabetes-induced breakdown of the BRB, implying that diabetes-induced retinal vascular disorders, such as diabetic macular edema or diabetic retinopathy, are a new indication for apatinib.

Materials and methods

Preparation of Apa-HSA-PEG nanoparticles

For the synthesis of HSA-PEG conjugates, 75 mg of *N*-hydroxysuccinimide-derivatized methoxy PEG (mPEG-NHS, molecular weight [MW] 5,000 Da, SunBio, Anyang, Korea) dissolved in phosphate-buffered saline (PBS) was added slowly to a solution containing 100 mg of HSA (Sigma-Aldrich, St Louis, MO, USA) with stirring. The stoichiometric feed ratio (mPEG-NHS:HSA) was 20:1. After incubation at room temperature (RT) for 12 hours, the reaction mixture was dialyzed in deionized water to remove unreacted PEG, freeze-dried, and stored at -20°C until use. The conjugate was analyzed using gel permeation chromatography (GPC). GPC was performed using a Waters 626 high performance liquid chromatography (HPLC) pump equipped with a Waters 486 UV detector and a PL aquagel OH mixed column (Agilent 1100s; Agilent Technologies, Santa Clara, CA, USA). The mobile phase was PBS flowing at a rate of 1 mL/min.

For the preparation of apatinib-loaded HSA-PEG (Apa-HSA-PEG) nanoparticles, HSA-PEG conjugates and apatinib (LSK Biopharma, Salt Lake City, UT, USA) were dissolved in 50% aqueous tetrahydrofuran and stirred for 30 minutes at RT. After evaporating the solvent using a rotary evaporator at 100°C under reduced pressure, the film containing HSA-PEG conjugates and apatinib was rehydrated in deionized water and dispersed into self-assembled nanoparticles by sonication. The resulting solution was filtered through a $0.8\ \mu\text{m}$ cellulose acetate filter unit and lyophilized to obtain a homogeneous white powder. Apa-HSA-PEG nanoparticles were reconstructed, when required, by dissolving the lyophilized product in PBS.

Characterization of Apa-HSA-PEG nanoparticles

The morphology of Apa-HSA-PEG nanoparticles was observed using a transmission electron microscope (TEM). The nanoparticles in deionized water were dropped onto a 300-mesh carbon-coated copper grid and dried at RT. The grid was stained with 2% uranyl acetate and observed under a TEM (JEM-3010; JEOL, Tokyo, Japan). The hydrodynamic size was determined using light-scattering method (Zeta Plus; Brookhaven Instruments, Holtsville, NY, USA) with a helium–neon laser at a wavelength of 632 nm and a 90° detection angle. The apatinib-loading content and apatinib-loading efficiency into HSA-PEG nanoparticles were determined using a Waters 626 HPLC pump equipped with a Waters 486 UV detector and a LiChrospher 100 RP-18 column (EMD Millipore, Billerica, MA, USA) with an acetonitrile–water (45:55, v/v) mobile phase at a flow rate of 0.5 mL/min.

Cell culture

Human retinal microvascular endothelial cells (HRMECs) were obtained from Cell Systems (Kirkland, WA, USA) and cultured in endothelial growth medium-2 (EGM-2; Lonza, Walkersville, MD, USA) at 37°C in a humidified incubator from passages three to six.

Cytotoxicity assay

HRMECs were seeded at a density of 2,000 cells/well in a 96-well plate. After 24-hour incubation in EGM-2, cells were treated with fresh EGM-2 containing apatinib (dissolved in dimethyl sulfoxide) or Apa-HSA-PEG nanoparticles for 1–2 days. Cell viability was evaluated using the Cell Counting Kit-8 assay (Dojindo Molecular Technology, Rockville, MD, USA) according to the manufacturer's protocol. The absorbance of each well was measured at 450 nm

using a microplate reader (BioTek Instruments, Winooski, VT, USA).

Endothelial paracellular permeability assay

HRMECs were seeded onto a gelatin (Sigma-Aldrich)-coated transwell membrane (Corning Incorporated, Corning, NY, USA) and cultured in EGM-2 to form a confluent monolayer. Paracellular permeability was assessed using fluorescein isothiocyanate (FITC)-conjugated dextran (MW 40,000 Da; Sigma-Aldrich) as described previously.¹⁰ Briefly, specified reagents were added with the endothelial basal medium (EBM; Lonza) to the upper transwell chamber. FITC-dextran was then added to the upper chamber at a final concentration of 1 mg/mL. After incubation for 30 minutes, fluorometric signals derived from FITC-dextran in the upper and lower chambers were measured using a fluorometer (BioTek Instruments).

Measurement of transendothelial electrical resistance

Electrical resistance across a monolayer of HRMECs cultured on the transwell membrane was measured using a Millicell ERS-2 Volt ohmmeter (EMD Millipore). Recombinant human VEGF (rhVEGF; Prospect Biosystems, Newark, NJ, USA) and/or Apa-HSA-PEG nanoparticles were added to the upper chamber at time zero, and changes in electrical resistance were measured 30 and 60 minutes later. Transendothelial electrical resistance (TEER) values were calculated by subtracting the background from the experimental TEER, and then multiplying the result by the surface area of the filter.

VE-cadherin internalization assay

The VE-cadherin internalization assay was performed according to a protocol described previously.¹⁰ Briefly, confluent HRMECs were incubated with anti-VE-cadherin IgG (R&D Systems, Inc., Minneapolis, MN, USA) at 4°C. After 1-hour incubation, unbound anti-VE-cadherin IgG was removed by washing the cells with cold EBM. Next, the cells were treated with EBM supplemented with rhVEGF and/or Apa-HSA-PEG nanoparticles at 37°C for 30 minutes, and washed with acidic PBS (pH 2.7, 25 mM glycine, 2% bovine serum albumin) to remove membrane-bound IgG for the quantification of internalized VE-cadherin. The cells with or without acid washes were fixed, blocked, and stained with FITC-conjugated secondary IgG (Molecular Probes, Eugene, OR, USA). For the co-immunofluorescence assay, the cells were further stained with primary IgG against early

endosome antigen 1 (EEA1) (BD Biosciences, San Jose, CA, USA) or ZO1 (BD Pharmingen, San Diego, CA, USA), followed by a rhodamine-conjugated secondary IgG (Molecular Probes). Cell nuclei were counterstained with 4',6-diamidino-2-phenylindole. The amount of internalized VE-cadherin was assessed by counting the number of acid-resistant VE-cadherin-positive vesicles per cell.

Animals

Animal experiments were conducted with 6- to 8-week-old C57BL/6 mice (Orient, Seoul, Korea). All animal protocols were reviewed and approved by the Chung-Ang University Institutional Animal Care and Use Committee in accordance with the Guide for the Care and Use of Laboratory Animals published by the National Institutes of Health (Bethesda, MD, USA). For intravitreal injection, mice were anesthetized with an intraperitoneal injection of ketamine/xylazine (120/16 mg/kg). The adequacy of anesthesia was assessed by monitoring the pedal withdrawal reflex response. At the conclusion of the experiments, animals were euthanized using carbon dioxide inhalation, and tissues were collected immediately for further analysis.

Retinal vascular permeability assay

Retinal vascular permeability was examined by fluorescein angiography and the Evans Blue (EB; Sigma-Aldrich) assay. Briefly, rhVEGF and/or Apa-HSA-PEG nanoparticles prepared in 1 µL PBS were injected into the vitreous cavity of one eye of each mouse, with an equal volume of PBS injected into the contralateral eye. For angiography, FITC-dextran (MW 40,000 Da; Sigma-Aldrich) was injected intravenously, and the mice were sacrificed 30 minutes later. The eyes were enucleated and fixed in 10% formalin (Sigma-Aldrich). The retinas were then prepared as flat mounts on glass slides and viewed with a fluorescence microscope (Nikon, Melville, NY, USA) in four randomly selected areas of each retina as described previously.¹⁰ For quantification of vascular leakage, 150 µL of EB (20 mg/mL in PBS, sonicated and filtered) was injected intravenously, and the mice were sacrificed 4 hours later. Two hundred microliters of blood was obtained, and the retinas were collected, dried, and weighed. EB was extracted from the dried retinas with formamide (Sigma-Aldrich) at 78°C overnight. The absorbance of the EB dye in blood and retinal tissues was measured at 620 and 740 nm using a spectrophotometer (BioTek Instruments). The amount of EB dye was calculated from a standard curve of EB in formamide. EB permeation was calculated as follows: [retinal EB amount/retinal weight]/[blood EB

concentration \times circulation time]. EB permeation of treated eyes was normalized relative to that of each contralateral PBS control.

Murine model of streptozotocin-induced diabetes

Six- to 8-week-old C57BL/6 mice were injected intraperitoneally with five consecutive daily doses of streptozotocin (STZ; 55 mg/kg; Sigma-Aldrich) freshly dissolved in 50 mM sodium citrate buffer (pH 4.5). Serum glucose levels were measured using an Accu-Check Advantage glucometer (Hoffman-La Roche Ltd., Basel, Switzerland) under nonfasting conditions. Mice with plasma glucose levels >300 mg/dL were considered as having STZ-induced diabetes. Two weeks after the initial STZ injection, Apa-HSA-PEG nanoparticles in 1 μ L of PBS were injected into the vitreous cavity of one eye. An equal volume of PBS was injected into the contralateral eye. One day later, retinal vascular permeability was assessed using the EB assay as described earlier.

Statistical analysis

All data are presented as mean values \pm standard errors of the means. One-way analysis of variance followed by Bonferroni's post hoc multiple comparison test was used to determine differences between multiple groups. $P < 0.05$ was considered as statistically significant. The number of samples in each experiment is indicated by n.

Results and discussion

Apa-HSA-PEG nanoparticles inhibit VEGF-mediated hyperpermeability in HRMECs

The HSA-PEG conjugate was synthesized by conjugating mPEG-NHS (MW 5,000 Da) to the primary amines of HSA. The average molecular weight of the conjugate was 125 kDa, suggesting that about 12 PEG molecules were conjugated to one HSA molecule, as determined by GPC analysis (data not shown). The preparation of Apa-HSA-PEG nanoparticles is presented schematically in Figure 1A.

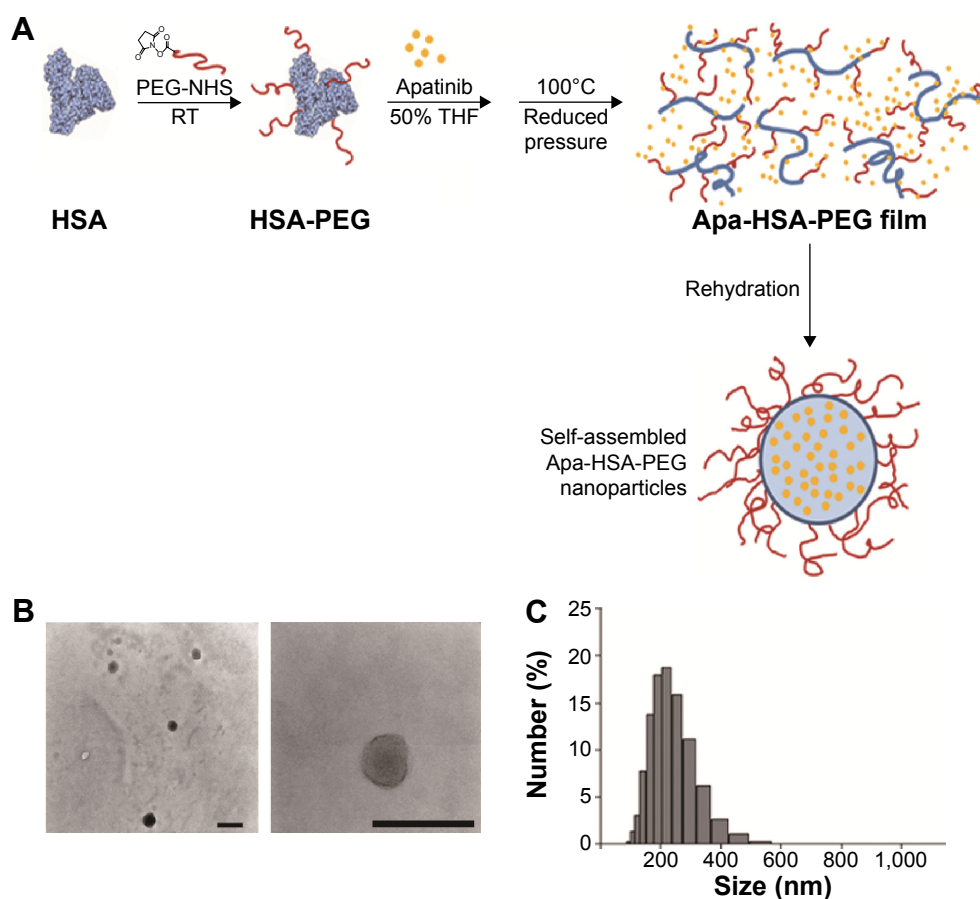


Figure 1 Preparation and characterization of Apa-HSA-PEG nanoparticles.

Notes: (A) Schematic diagram of the preparation of Apa-HSA-PEG nanoparticles. (B) TEM images and (C) particle size distribution of Apa-HSA-PEG nanoparticles. All scale bars = 500 nm.

Abbreviations: Apa-HSA-PEG, apatinib-loaded human serum albumin-conjugated polyethylene glycol; TEM, transmission electron microscope; NHS, N-hydroxysuccinimide; RT, room temperature; THF, tetrahydrofuran.

The HSA-PEG conjugate and apatinib were dissolved in a 50% tetrahydrofuran aqueous solution. The solvent was then evaporated under reduced pressure at 100°C, forming a thin and transparent film. Apa-HSA-PEG nanoparticles were generated by dissolving the film in deionized water. The nanoparticles showed spherical morphology with a diameter of 267.5 ± 0.97 nm (Figure 1B and C). High-performance liquid chromatography analysis revealed that the loading amount and entrapping efficiency of Apa-HSA-PEG nanoparticles were 5.4 (w/w) and 77.1%, respectively.

We first determined the cytotoxicity of Apa-HSA-PEG nanoparticles in HRMECs. Apa-HSA-PEG nanoparticles did not compromise the viability of HRMECs (Figure 2A).

We then evaluated the inhibitory effect of Apa-HSA-PEG nanoparticles on VEGF-induced hyperpermeability in HRMECs. VEGF significantly enhanced the passage of FITC-labeled dextran across the HRMEC monolayer (Figure 2B). At a noncytotoxic concentration (1 μ M on an apatinib basis), Apa-HSA-PEG nanoparticles completely inhibited VEGF-induced endothelial hyperpermeability. The inhibitory effect of Apa-HSA-PEG nanoparticles was similar to that of free apatinib solution at the same concentration. The TEER assay also demonstrated the ability of Apa-HSA-PEG nanoparticles to block the VEGF-mediated decrease in electrical resistance across the HRMEC monolayer (Figure 2C).

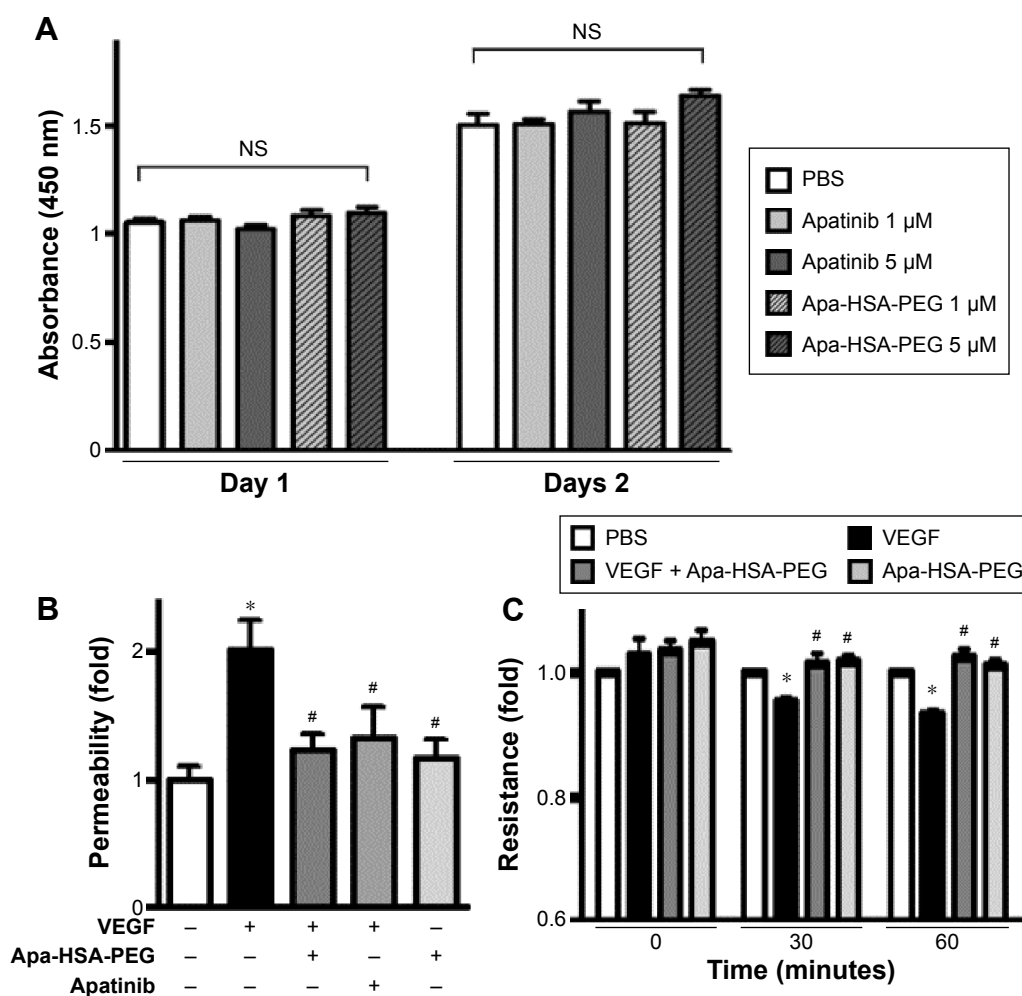


Figure 2 Apa-HSA-PEG nanoparticles block VEGF-induced hyperpermeability in HRMECs.

Notes: (A) Cytotoxicity of Apa-HSA-PEG nanoparticles and apatinib was evaluated using the Cell Counting Kit-8 assay (n=6). HRMECs were incubated with apatinib (1 and 5 μ M) or Apa-HSA-PEG nanoparticles (960 and 4.8 μ g corresponding to 1 and 5 μ M apatinib, respectively) for 1–2 days. (B and C) Endothelial permeability was evaluated by measuring the (B) passage of FITC-dextran and (C) TEER in a HRMEC monolayer. HRMECs pretreated with apatinib (1 μ M) or Apa-HSA-PEG nanoparticles (6.1 μ g corresponding to 1 μ M apatinib), and untreated cells were stimulated with rhVEGF (50 ng/mL). (B) FITC-dextran permeability is expressed as the fold change \pm SEM with respect to the PBS control (* P <0.05 vs PBS control, # P <0.05 vs VEGF, n=6). (C) In the TEER experiment, specified reagents were added to the upper chamber at time zero, and serial changes in electrical resistance were measured 30 and 60 minutes later. Electrical resistance is expressed as the fold change \pm SEM relative to the PBS control at each time point (* P <0.05 vs PBS control, # P <0.05 vs VEGF, n=6).

Abbreviations: Apa-HSA-PEG, apatinib-loaded human serum albumin-conjugated polyethylene glycol; VEGF, vascular endothelial growth factor; HRMECs, human retinal microvascular endothelial cells; FITC, fluorescein isothiocyanate; TEER, transendothelial electrical resistance; rhVEGF, recombinant human VEGF; SEM, standard error of the mean; PBS, phosphate-buffered saline; NS, nonsignificant.

Because VEGF-induced increases in endothelial paracellular permeability occur through the breakdown of adherens junctions composed of VE-cadherin, we investigated whether Apa-HSA-PEG nanoparticles prevented VEGF-induced internalization of VE-cadherin in HRMECs. VEGF treatment resulted in the loss of VE-cadherin at endothelial cell–cell junctions that are co-aligned with the tight junction protein, ZO1 (Figure 3). In addition, accumulation of acid wash-resistant intracellular VE-cadherin was colocalized with the early endosomal marker, EEA1. This VEGF-induced internalization of VE-cadherin was almost completely blocked by treatment with Apa-HSA-PEG nanoparticles. These results indicate that Apa-HSA-PEG nanoparticles efficiently block the VEGF-induced endothelial

hyperpermeability and internalization of VE-cadherin in HRMECs.

Apa-HSA-PEG nanoparticles block the VEGF-induced increase in retinal vascular leakage in vivo

To further demonstrate the role of Apa-HSA-PEG nanoparticles in VEGF-triggered vascular leakage, we performed an in vivo retinal vascular permeability assay with intravitreal injection of VEGF and/or Apa-HSA-PEG nanoparticles (Figure 4A). VEGF treatment induced substantial leakage of systemically injected FITC-dextran in the retinal vasculature with consequent perivascular hyperfluorescence. However, co-injection of Apa-HSA-PEG

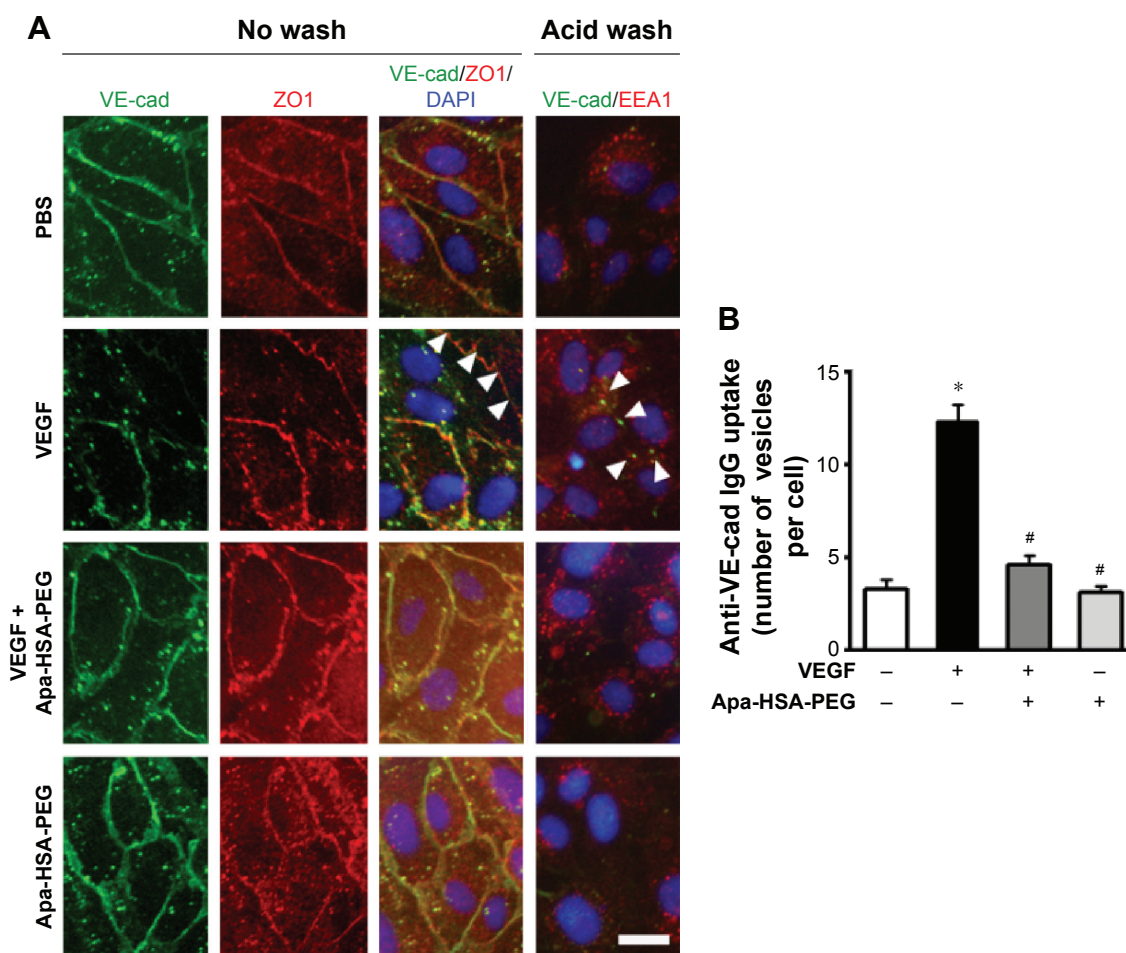


Figure 3 Apa-HSA-PEG nanoparticles prevent VEGF-induced internalization of VE-cadherin.

Notes: (A) Representative immunofluorescent images of VE-cadherin. (B) Quantification of internalized VE-cadherin in HRMECs (means \pm SEM, * $P < 0.05$ vs PBS, # $P < 0.05$ vs VEGF, $n = 4$). Cells pretreated with Apa-HSA-PEG nanoparticles (6.1 μ g corresponding to 1 μ M apatinib) or PBS were stimulated with rhVEGF (50 ng/mL). Arrowheads in the no wash image indicate the disappearance of VE-cadherin (green) at endothelial junctions that were stained positively for anti-ZO1 IgGs (red). Arrowheads in the acid wash image indicate internalized VE-cadherin (green) in endosomes that were stained positively for EEA1 (red). Nuclei are shown in blue (DAPI). Scale bars = 25 μ m.

Abbreviations: Apa-HSA-PEG, apatinib-loaded human serum albumin-conjugated polyethylene glycol; EEA1, early endosome antigen 1; VEGF, vascular endothelial growth factor; VE, vascular endothelial; HRMECs, human retinal microvascular endothelial cells; SEM, standard error of the mean; PBS, phosphate-buffered saline; rhVEGF, recombinant human VEGF; DAPI, 4',6-diamidino-2-phenylindole; VE-cad, VE-cadherin.

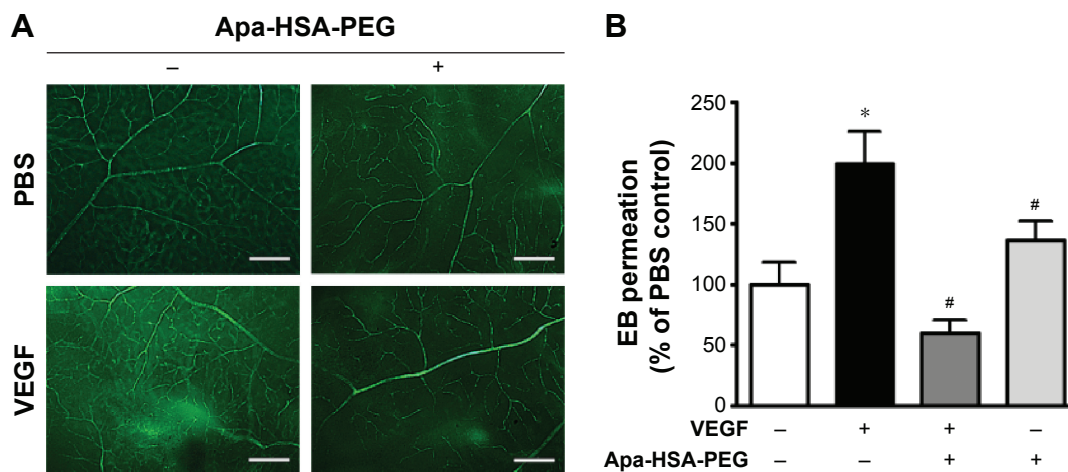


Figure 4 Apa-HSA-PEG nanoparticles block VEGF-induced retinal vascular leakage in vivo.

Notes: (A) Representative images of FITC-dextran-perfused retinal whole mounts. (B) Quantitative analysis of extravasated EB dye in the retinal tissues after intravitreal injection of rhVEGF (100 ng) and/or Apa-HSA-PEG nanoparticles (580 ng). Vascular leakage of EB dye in treated eyes was normalized relative to that in each contralateral control eye (means \pm SEM, * $P < 0.05$ vs PBS control, # $P < 0.05$ vs VEGF, $n = 5$). Scale bar = 200 μ m.

Abbreviations: Apa-HSA-PEG, apatinib-loaded human serum albumin-conjugated polyethylene glycol; VEGF, vascular endothelial growth factor; FITC, fluorescein isothiocyanate; EB, Evans Blue; rhVEGF, recombinant human VEGF; SEM, standard error of the mean; PBS, phosphate-buffered saline.

nanoparticles and VEGF resulted in a significant inhibition of VEGF-induced extravasation of FITC-dextran. Quantification analyses of retinal vascular leakage using EB dye showed an approximately twofold increase of EB deposition in VEGF-treated retinal tissues. This increase was significantly reduced by treatment with Apa-HSA-PEG nanoparticles (Figure 4B). These data support that Apa-HSA-PEG nanoparticles effectively prevent VEGF-induced disruption of the BRB in vivo.

Intravitreal injection of Apa-HSA-PEG nanoparticles inhibits retinal vascular leakage in STZ-injected diabetic mice

VEGF has been considered as a primary factor in the pathogenesis of diabetes-induced retinal vascular diseases. Because increased expression of VEGF contributes to early retinal vascular hyperpermeability and subsequent macular edema during the progression of diabetic retinopathy and diabetic macular edema, we determined whether Apa-HSA-PEG nanoparticles could inhibit diabetes-induced retinal vascular hyperpermeability using STZ-induced diabetic mice. Two weeks after STZ injection, diabetic mice with elevated serum glucose levels (>300 mg/dL) and reduced body weights were selected and intravitreally injected with Apa-HSA-PEG nanoparticles or PBS. Vascular leakage of EB in Apa-HSA-PEG nanoparticles-injected retinas was significantly lower than that of the PBS-injected contralateral controls (Figure 5A). Serum glucose levels and body weights

of mice used in this experiment were measured before and after STZ injection (Figure 5B).

Conclusion

Visual impairment and blindness are leading health care issues worldwide with substantial socioeconomic consequences. In particular, the high prevalence of diabetes and obesity has increased concerns over diabetic eye diseases such as retinopathy and macular edema. Treatment and management of such diseases are challenging owing to anatomical and physiological characteristics of the eye which limit the entry of drugs from the blood to the retina and vitreous cavity. To improve drug bioavailability, nanotechnology is being employed in several ophthalmic applications for retinal and choroidal vascular disorders.¹¹ For example, Ozurdex[®], a biodegradable dexamethasone implant composed of polylactic-co-glycolic acid, is being used for patients with diabetic macular edema or macular edema associated with uveitis. Iluvien[®], a nonerodible polyimide implant that releases fluocinolone acetonide, was also recently approved for the treatment of diabetic macular edema. Corticosteroids, such as dexamethasone and fluocinolone acetonide, are efficacious in inhibiting inflammation, edema, angiogenesis, and fibrosis. However, their low solubility in water often causes the early exclusion from, or accumulation of, drug in ocular tissues, resulting in local toxicity, elevated intraocular pressure, and optic nerve degeneration.^{12,13} Therefore, improved drug carriers are required for effective ocular delivery of

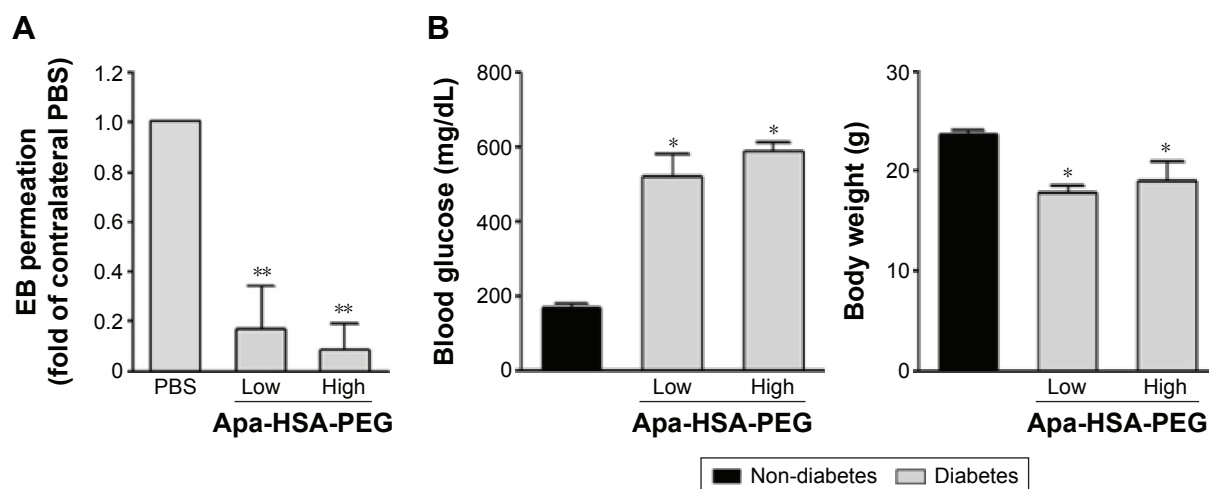


Figure 5 Intravitreal injection of Apa-HSA-PEG nanoparticles inhibits diabetes-induced retinal vascular leakage in STZ-induced diabetic mice.

Notes: (A) STZ-induced diabetic mice received an intravitreal injection of Apa-HSA-PEG nanoparticles (61 ng for the low-dose group [Low], 610 ng for the high-dose group [High]). An equal volume of PBS was injected into the contralateral eye as a control. One day after injection, retinal vascular leakage of EB dye was measured and expressed relative to that in each contralateral control eye (means \pm SEM, $**P < 0.01$ vs contralateral PBS control, $n=8$). (B) Blood glucose and body weights of mice used in this experiment were measured before (Nondiabetes) and 2 weeks after (Diabetes) the initial STZ injection ($*P < 0.05$ vs Nondiabetes, $n=8$).

Abbreviations: Apa-HSA-PEG, apatinib-loaded human serum albumin-conjugated polyethylene glycol; STZ, streptozotocin; PBS, phosphate-buffered saline; EB, Evans Blue; SEM, standard error of the mean.

poorly water-soluble drugs while reducing toxicity, compared to the free drug.

For intravitreal injection of water-insoluble apatinib, HSA-PEG nanoparticles were used as the drug delivery system in the present study. Among various types of nanoparticle materials, HSA-PEG has several advantages as a drug delivery carrier. Specifically, HSA is an endogenous protein located primarily in the blood and has a native role as a plasma protein carrier. This makes HSA a safe biomaterial for delivering hydrophobic drugs. In addition, HSA increases drug solubility, protects drugs against oxidation, and enhances the drug half-life.^{11,14} Indeed, an HSA-based formulation of the water-insoluble anticancer drug, paclitaxel, was approved by the US Food and Drug Administration and has been used for treating breast and pancreatic cancers.¹⁵ In the present study, HSA was conjugated with PEG, a widely used polymer, for improving the solubility and biocompatibility of the drug delivery system. PEGylated HSA exhibits enhanced solubility in aqueous or protic solvents, allowing a simple oil-free fabrication of nanoparticles containing hydrophobic drugs such as apatinib. Nanoparticles prepared with PEGylated HSA may be safe and less prone to have formulation-related toxicity in vivo.

To our knowledge, this is the first study demonstrating the therapeutic potential of the anticancer drug, apatinib, in the treatment of diabetes-induced retinal vascular disorders by using HSA-PEG nanoparticles as a drug delivery carrier. In vitro and in vivo experiments revealed that Apa-HSA-PEG

nanoparticles efficiently blocked VEGF-induced retinal vascular hyperpermeability. In addition, intravitreal injection of these nanoparticles substantially inhibited diabetes-induced retinal vascular leakage in a diabetic mouse model. The results of this study suggest that apatinib may provide a novel therapy for diabetic retinopathy or diabetic macular edema when delivered intravitreally via HSA-PEG nanoparticles.

Acknowledgments

This work was supported by the National Research Foundation of Korea (NRF) grants funded by the Korean government (MSIP)(2013R1A2A2A04016796, 2015R1A2A1A15052509, and 2015R1D1A1A02061724).

Disclosure

The authors report no conflicts of interest in this work.

References

1. Klaassen I, Van Noorden CJ, Schlingemann RO. Molecular basis of the inner blood-retinal barrier and its breakdown in diabetic macular edema and other pathological conditions. *Prog Retin Eye Res.* 2013;34:19–48.
2. Aiello LP, Avery RL, Arrigg PG, et al. Vascular endothelial growth factor in ocular fluid of patients with diabetic retinopathy and other retinal disorders. *N Engl J Med.* 1994;331:1480–1487.
3. Weis SM, Cherech DA. Pathophysiological consequences of VEGF-induced vascular permeability. *Nature.* 2005;437:497–504.
4. Dejana E, Tournier-Lasserre E, Weinstein BM. The control of vascular integrity by endothelial cell junctions: molecular basis and pathological implications. *Dev Cell.* 2009;16:209–221.

5. Ho AC, Scott IU, Kim SJ, et al. Anti-vascular endothelial growth factor pharmacotherapy for diabetic macular edema: a report by the American Academy of Ophthalmology. *Ophthalmology*. 2012;119:2179–2188.
6. Roviello G, Ravelli A, Polom K, et al. Apatinib: a novel receptor tyrosine kinase inhibitor for the treatment of gastric cancer. *Cancer Lett*. 2016; 372:187–191.
7. Tian S, Quan H, Xie C, et al. YN968D1 is a novel and selective inhibitor of vascular endothelial growth factor receptor-2 tyrosine kinase with potent activity in vitro and in vivo. *Cancer Sci*. 2011;102:1374–1380.
8. Li J, Qin S, Xu J, et al. Apatinib for chemotherapy-refractory advanced metastatic gastric cancer: results from a randomized, placebo-controlled, parallel-arm, phase II trial. *J Clin Oncol*. 2013;31:3219–3225.
9. Li J, Zhao X, Chen L, et al. Safety and pharmacokinetics of novel selective vascular endothelial growth factor receptor-2 inhibitor YN968D1 in patients with advanced malignancies. *BMC Cancer*. 2010;10:529.
10. Kim JY, Choi JS, Song SH, et al. Stem cell factor is a potent endothelial permeability factor. *Arterioscler Thromb Vasc Biol*. 2014;34:1459–1467.
11. Kompella UB, Amrite AC, Pacha Ravi R, Durazo SA. Nanomedicines for back of the eye drug delivery, gene delivery, and imaging. *Prog Retin Eye Res*. 2013;36:172–198.
12. Diebold Y, Calonge M. Applications of nanoparticles in ophthalmology. *Prog Retin Eye Res*. 2010;29:596–609.
13. Xu Q, Kambhampati SP, Kannan RM. Nanotechnology approaches for ocular drug delivery. *Middle East Afr J Ophthalmol*. 2013;20:26–37.
14. Kragh-Hansen U, Chuang VT, Otagiri M. Practical aspects of the ligand-binding and enzymatic properties of human serum albumin. *Biol Pharm Bull*. 2002;25:695–704.
15. Sparreboom A, Scripture CD, Trieu V, et al. Comparative preclinical and clinical pharmacokinetics of a cremophor-free, nanoparticle albumin-bound paclitaxel (ABI-007) and paclitaxel formulated in Cremophor (Taxol). *Clin Cancer Res*. 2005;11:4136–4143.

International Journal of Nanomedicine

Publish your work in this journal

The International Journal of Nanomedicine is an international, peer-reviewed journal focusing on the application of nanotechnology in diagnostics, therapeutics, and drug delivery systems throughout the biomedical field. This journal is indexed on PubMed Central, MedLine, CAS, SciSearch®, Current Contents®/Clinical Medicine,

Submit your manuscript here: <http://www.dovepress.com/international-journal-of-nanomedicine-journal>

Dovepress

Journal Citation Reports/Science Edition, EMBase, Scopus and the Elsevier Bibliographic databases. The manuscript management system is completely online and includes a very quick and fair peer-review system, which is all easy to use. Visit <http://www.dovepress.com/testimonials.php> to read real quotes from published authors.